Micellar structure changes in aqueous mixtures of nonionic surfactants

Liang Guo and Ralph H. Colby[a)]

Materials Science and Engineering, The Pennsylvania State University, University Park, Pennsylvania 16802

Min Y. Lin

Center for Neutron Research, National Institute of Standards and Technology, Gaithersburg, Maryland 20899

Gregory P. Dado[b)]

Air Products and Chemicals, Inc., Allentown, Pennsylvania 18195

(Received 7 February 2001; final revision received 22 May 2001)

Synopsis

Rheology and small-angle neutron scattering are used to probe the structure of nonionic surfactant mixtures in water. Small amounts of a C_{14} diol (Surfynol® 104) cause enormous structural and rheological changes when added to aqueous solutions of an ethylene oxide-propylene oxide-ethylene oxide triblock copolymer (Pluronic® P105). The C_{14} diol is only soluble up to 0.1 wt % in pure water, but can be added in large quantities to aqueous solutions of the copolymer. The hydrophobic diol incorporates into the existing copolymer micelles and causes a cascade of changes in the micelle structure, with resultant changes in rheology. Particularly striking is the spherical to worm-like micelle transition, where the viscosity changes by a factor of more than 10^4. © *2001 The Society of Rheology.* [DOI: 10.1122/1.1389315]

I. INTRODUCTION

Water-soluble triblock copolymers of poly(ethylene oxide) and poly(propylene oxide), often denoted PEO–PPO–PEO, are commercially available nonionic macromolecular surfactants commonly known as Poloxamers® (manufactured by ICI) or Pluronics® (manufactured by BASF). Tailoring the copolymer composition and molecular weight in the manufacturing process results in a wide range of products with optimum properties suitable for use in a variety of industrial areas. As a result, PEO–PPO–PEO copolymers have found widespread industrial applications in such areas as detergency, foaming/defoaming, emulsification, dispersion stabilization, lubrication, as well as some more special application fields as cosmetics, pharmaceuticals, and bioprocessing [Alexandridis and Hatton (1995); Chu (1995)].

[a)]Author to whom all correspondence should be addressed. Electronic mail: rhc@plmsc.psu.edu
[b)]Current address: Stepan Company, Northfield, IL 60093.

Owing to the application potential of PEO–PPO–PEO copolymers in such widespread important areas, this product family has remained an active research topic in recent years. Aqueous solutions of these copolymers have been studied extensively. The kinetics and thermodynamics of micellization have been studied, including the effects of temperature and system composition on the micelle structure [Zhou and Chu (1988); Nagarajan and Ganesh (1989a and 1989b); Wanka *et al.* (1990); Brown *et al.* (1991); Brown *et al.* (1992); Mortensen and Brown (1993a); Mortensen and Pedersen (1993b); Wanka *et al.* (1994); Alexandridis *et al.* (1994); Prud'homme *et al.* (1996); Nagarajan (1999)].

In contrast to the extensive work on PEO–PPO–PEO copolymers in water, their interactions with additives have been less probed and only a few publications are available [Almgren *et al.* (1991a and 1991b); Bahadur *et al.* (1993); Hecht and Hoffmann (1994 and 1995); Hecht *et al.* (1995); Jørgensen *et al.* (1997); Contractor and Bahadur (1998); Alexandridis *et al.* (2000); Bromberg *et al.* (2000); Guo *et al.* (2000); Ivanova *et al.* (2000a and 2000b); Plucktaveesak *et al.* (2000)]. As PEO–PPO–PEO copolymers find applications mostly in complex environments, studying effects of various additives can be useful for optimizing their applications. In this paper, we report our studies by rheology and small-angle neutron scattering (SANS) on complex aqueous mixtures of $(EO)_{37}(PO)_{56}(EO)_{37}$ and a hydrophobic nonionic C_{14} diol.

II. MICELLIZATION OF PEO–PPO–PEO TRIBLOCK COPOLYMERS

In a certain temperature range and at a certain copolymer concentration, PEO–PPO–PEO block copolymers of suitable composition and molecular weight form polymolecular aggregates (micelles) in an aqueous environment. SANS on $(EO)_{78}(PO)_{30}(EO)_{78}$ aqueous solutions [Zhou and Chu (1988)] shows a transition at the critical micellization temperature (CMT). Below the CMT, a small particle size of unimers (2.3 nm) is observed with very little temperature dependence. Micelle formation becomes appreciable above the CMT. In the micelle region, the measured micellar mass increases linearly with temperature, while the hydrodynamic radius of the micelles remains nearly constant (8.0 nm). $(EO)_{13}(PO)_{30}(EO)_{13}$ shows detectable aggregates at 25 °C when the concentration is above approximately 6% [Al-Saden *et al.* (1982)]. The micelle size increases with concentration (10 nm at 8%–12.5 nm at 20%) and exhibits significant polydispersity. At 35 °C, however, essentially invariant values for the hydrodynamic radius are found over a wide concentration range and the micelles are roughly monodisperse. Mortensen and co-workers (1992a, 1992b, 1993a, 1993b) found that the radius of gyration of the free copolymers (unimers) is 1.7 nm. The micellar sizes (micelle core radius and hard-sphere interaction radius) are independent of polymer concentration, but show small temperature dependence reflecting a change in aggregation number. The micelle core radius and hard-sphere interaction radius are 3.8 and 6.0 nm at 20 °C, respectively, and increase to 5.1 and 7.5 nm at 50 °C. The SANS results of Yang and Alexandridis (2000a) on 2.5 wt % $(EO)_{13}(PO)_{30}(EO)_{13}$ in aqueous (D_2O) solution show that the micelles are well separated while the intermicellar interaction remains strong and a core-shell model is more appropriate for the micelle morphology. Upon an increase of temperature in the range 35–55 °C, the micelle radius increases by about 10%, accompanied by the loss of water in the micelle core.

In the analysis of SANS intensity distributions from $(EO)_{19}(PO)_{43}(EO)_{19}$ and $(EO)_{27}(PO)_{61}(EO)_{27}$ micelles in aqueous solutions, Liu and co-workers (1998) proposed a ''cap-and-gown'' model for the microstructure of the micelles, taking into consideration the polymer segmental distribution and water penetration profile in the core and corona

regions, coupled with an adhesive hard-sphere model for describing the intermicellar interactions. The structure of micelles stays essentially constant as a function of concentration, but changes rapidly with temperature. The micellar core is not completely dry but contains up to 20% volume fraction of solvent molecules at low temperatures (35 °C). The aggregation number increases, but the micelle contains less water with increasing temperature. Contrasting the two polymers suggests that micelles formed by a polymer with higher molecular weight tend to carry a larger volume fraction of solvent molecules.

Studies on $(EO)_{27}(PO)_{39}(EO)_{27}$, $(EO)_{67}(PO)_{39}(EO)_{67}$, and $(EO)_{96}(PO)_{39}(EO)_{96}$ revealed complex states of aggregation in solution [Brown *et al.* (1992)]. Unimer, micelles, and larger aggregated clusters coexist and their fractions depend strongly on temperature and concentration. The unimers have hydrodynamic radii in the range of 1.5–3.0 nm; the micelle radii are 8–13 nm (in sequence of increasing PEO block length), whereas the radii of the clusters are greater than 80 nm. Mortensen and Brown (1993a) found that the PPO concentration is the relevant parameter that determines the CMT. The micellar core radius, R_C, is essentially independent of copolymer concentration but shows a significant increase with temperature. When R_C is plotted against reduced temperature $T-T_{\mathrm{CMT}}$, the data for solutions of the three copolymers fall on a common master curve following an empirical scaling relation $R_C \sim (T-T_{\mathrm{CMT}})^{0.2}$. In the studies of Brown and coworkers (1992), oscillatory shear rheological measurements were also utilized in combination with dynamic light scattering (DLS) and SANS techniques to probe the gelation process with increasing temperature for the three copolymers at high concentrations. Aqueous solutions of all three copolymers are liquids (i.e., $G'' \gg G'$) at low temperatures and gel at elevated temperatures (where G' increases by several orders of magnitude and becomes much larger than G''). When the temperature is increased further, G' passes through a maximum and eventually drops to values smaller than G''. The entire process of gel formation and dissolution at different temperatures is thermally reversible, showing very little hysteresis. Their DLS and SANS results indicate that the gel consists of close-packed micelles.

Prud'homme and co-workers (1996) also used rheometry together with SANS to examine the gelation and gel structure of $(EO)_{100}(PO)_{65}(EO)_{100}$ in water. At copolymer concentrations of less than 12.5%, the solutions are Newtonian liquids over a wide temperature range from 10 to 75 °C. For higher concentration samples ($c \geqslant 15\%$), the fluids are non-Newtonian over an intermediate temperature range that becomes wider with increasing polymer concentration. The 15% sample is Newtonian for temperatures $\leqslant 30$ or $\geqslant 50$ °C and non-Newtonian between 30 and 50 °C, reaching a viscosity maximum at ~ 40 °C. Gels with an ordered structure formed by cubic packing of spherical micelles are observed over a well-defined temperature window when the copolymer concentrations are greater than 17 wt %. Low yield stresses, very high zero shear viscosities, and shear thinning are the major rheological characteristics of the gels. The yield stress is due to repulsive interactions of PEO chains in the overlapped micellar shell. The transition between Newtonian and non-Newtonian behavior becomes more abrupt for higher solution concentrations. The sharp transition in the rheological data accompanies the structural order seen in the SANS measurements. The proposed gelation mechanism involves repulsive interactions among close packed spherical micelles, rather than aggregation or transitions in micelle morphology to rods or lamellae.

Hvidt and co-workers [Hvidt *et al.* (1994)] observed more complicated rheology in solutions of $(EO)_{21}(PO)_{47}(EO)_{21}$. At low concentrations ($< 24\%$) a soft gel is formed between 60 and 75 °C. Above 35%, these solutions form very rigid gels at all temperatures higher than 15 °C. However, at intermediate concentrations, a hard gel is formed at

low temperatures (20–45 °C) and a soft gel is formed at high temperatures (50–75 °C), with a liquid state being present in between (45–50 °C).

III. INTERACTION OF PEO–PPO–PEO TRIBLOCK COPOLYMERS WITH ADDITIVES

Jørgensen and co-workers [Jørgensen *et al.* (1997)] studied $(EO)_{27}(PO)_{39}(EO)_{27}$ with added inorganic salts. They examined four characteristic transitions: cloud points, sphere-to-rod transition temperature, soft gel formation temperature, and hard gel formation temperature at the critical gelation concentration. While the micellization and gelation of the copolymer in salt-containing solutions follow the same pattern as the salt-free system, the temperatures for cloud points, micellar sphere-to-rod transition, and gel formation are shifted with the salt addition. The cloud point shifts are in good agreement with previous measurements by Bahadur and co-workers [Bahadur *et al.* (1993)]. KF and KCl decrease the cloud point while the inorganic salt $K^+(CNS)^-$ gives a higher cloud point. The temperature shifts for the sphere-to-rod transition and the soft gel formation are equal to the temperature shifts in cloud point for the different salt types and the observed shifts are proportional to salt concentration. The temperatures of hard gel formation do not follow the same pattern, however. Different salts give different shifts and the shifts are inconsistent with the shifts in cloud point.

Hecht and Hoffmann (1994 and 1995) have investigated the influence of electrolytes and surfactants on the aggregation behavior of $(EO)_{100}(PO)_{39}(EO)_{100}$, $(EO)_{20}(PO)_{69}(EO)_{20}$ and $(EO)_{97}(PO)_{69}(EO)_{97}$. The micelle formation is influenced by the addition of both salts and surfactants. The CMT of the copolymers decreases linearly as salt is added, presumably reflecting a poorer solvent condition. Ionic surfactants strongly interact with PEO–PPO–PEO copolymers. Anionic surfactant sodium dodecyl sulfate (SDS) binds to monomers of $(EO)_{97}(PO)_{69}(EO)_{97}$ and can suppress completely the formation of copolymer micelles. At saturation, about six SDS molecules bind to one copolymer molecule. The peak observed in differential scanning calorimetry, associated with the CMT, decreases on the addition of SDS and eventually completely disappears [Hecht *et al.* (1995)]. SDS begins to aggregate with $(EO)_{100}(PO)_{39}(EO)_{100}$ at concentrations less than a quarter of its own CMC [Contractor and Bahadur (1998)]. SDS molecules strongly interact with the hydrophobic PPO core of $(EO)_{13}(PO)_{30}(EO)_{13}$ and $(EO)_{78}(PO)_{30}(EO)_{78}$ to form mixed micelles at temperatures lower than the CMT of the copolymers alone [Almgren *et al.* (1991a and 1991b)].

Recently, the ternary phase diagrams of $(EO)_{37}(PO)_{56}(EO)_{37}$ aqueous solutions with a variety of additives have been reported. The additives promote micellar structural changes, with three possible structures: spherical, worm-like, and lamellar micelles. Structure identification was performed with small-angle x-ray scattering. The additives studied were two esters (triacetin and propylene carbonate) [Ivanova *et al.* (2000a)], and ethanol, propylene glycol (a C_3 diol), glycerol (a C_3 triol), and glucose (a C_6 polyol) [Ivanova *et al.* (2000b); Alexandridis *et al.* (2000)]. Each additive produced a distinct ternary phase diagram, with extensive regions having multiple coexisting phases.

IV. EXPERIMENT

A. Materials

Pluronic® P105 was provided by BASF Corp. and Surfynol® 104 was supplied by Air Products and Chemicals, Inc. Both materials were used as received without further purification. The Pluronic® P105 is a triblock copolymer of the structure $(EO)_{37}(PO)_{56}(EO)_{37}$

with a waxy appearance at room temperature. It has a nominal molecular weight of 6500, composed of a center PPO block accounting for 50% of the mass and two identical PEO end blocks accounting for the other 50% of the mass. The Surfynol® 104 is a whitish solid material with a waxy appearance at room temperature and has very low solubility in water (roughly 0.1 wt %). It is a C_{14} diol with molecular weight of 226 and the following structure:

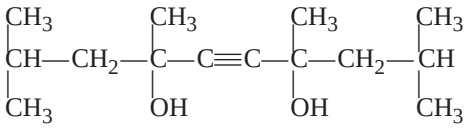

B. Equipment

Steady shear viscosity measurements were made using the Contraves LS 30 controlled shear rate rheometer with a concentric cylinder geometry. The cup diameter is 12.0 mm, while the bob has a diameter of 11.1 mm and a height of 8 mm. The dynamic measurements were performed using a Rheometric Scientific SR 2000 controlled stress rheometer with a cone and plate geometry. The cone has a diameter of 40 mm and cone angle of 0.0397 rad. In both rheometers, temperature is controlled using a circulating water bath to ± 0.1 °C.

Small-angle neutron scattering experiments were performed at the NIST Center for Neutron Research, Gaithersburg, MD. A combination of three instrumental setups was used to cover a q range from 0.0014 to 0.27 $Å^{-1}$. For the very low q range from 0.0014 to 0.005 $Å^{-1}$, the neutron wavelength used is 12 Å with a 15% full-width-at-half-maximum (FWHM) wavelength spread. The neutron source to sample distance is 16.32 m and the sample to detector distance is 13.10 m. The source aperture diameter is 25 mm and the sample diameter is 9.53 mm. For the low q range from 0.005 to 0.05 $Å^{-1}$, a neutron wavelength of 6 Å with a 15% FWHM wavelength spread is used. The neutron source-sample distance is 16.32 m and the sample-detector distance is 13.10 m. The source aperture diameter is 14.0 mm and the sample diameter is 9.53 mm. For the intermediate to high q range from 0.05 to 0.27 $Å^{-1}$, a 6 Å neutron wavelength with a 15% FWHM spread has been used. The neutron source to sample distance is 14.77 m and the sample to detector distance is 2.35 m. The source aperture diameter is 50 mm and the sample diameter is 9.53 mm. For data fitting with analytical models, smearing is applied to the whole q range with the earlier instrumental setups by using the resolution function $R(q,\langle q\rangle)$ developed by Pedersen and co-workers [Pedersen *et al.* (1990)]. We did not perform incoherent background scattering measurements. Hence, in our model fitting, the background scattering is *not* subtracted. Instead, we treated the background scattering as an adjustable q-independent parameter.

V. RESULTS AND DISCUSSION

The copolymer $(EO)_{37}(PO)_{56}(EO)_{37}$ is easily dissolved in water at room temperature. A 5 wt % stock solution of this copolymer in de-ionized distilled water was first prepared. The C_{14} diol has a low solubility in water (up to 0.1 wt %) but can be added to the copolymer solution in much larger amounts. Different amounts of C_{14} diol were added to the 5 wt % copolymer stock solution to prepare the samples studied. The samples were annealed at 80 °C for more than 30 minutes and then taken out of the oven and shaken for mixing. They were then annealed for another 30 minutes at 80 °C, followed by constant

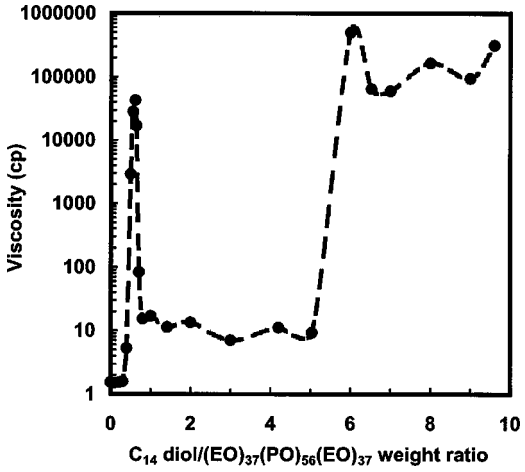

FIG. 1. Low shear rate (0.001 s^{-1}) viscosity at 25 °C for 5 wt % aqueous $(EO)_{37}(PO)_{56}(EO)_{37}$ solutions with the addition of C_{14} diol at different levels. The dashed line in the plot is meant for visual guidance.

shaking when taken out of the oven to cool down to room temperature. This heat treatment appears to accelerate the approach to equilibrium as detailed later.

Low shear rate (0.001 s^{-1}) viscosity was measured for the samples and the results are shown in Fig. 1. Here it can be seen that up to the diol/copolymer weight ratio of 0.3, all the samples show nearly an identical viscosity to that of 5 wt % copolymer in water (1.6 cp). Above the weight ratio of 0.3, the viscosity increases sharply and reaches a maximum at the weight ratio of 0.61. When the diol level increases further, the viscosity begins to drop significantly until the weight ratio of 0.80 is reached. In the diol/copolymer weight ratio range from 0.8 to 5, the viscosity is nearly constant at $\sim$ 10 cp. When the weight ratio reaches 6, the viscosity has another sharp increase and the solution has the consistency of a thick paste. Figure 2 shows the shear rate dependent apparent viscosity for the copolymer solutions with different amounts of diol added. The solutions

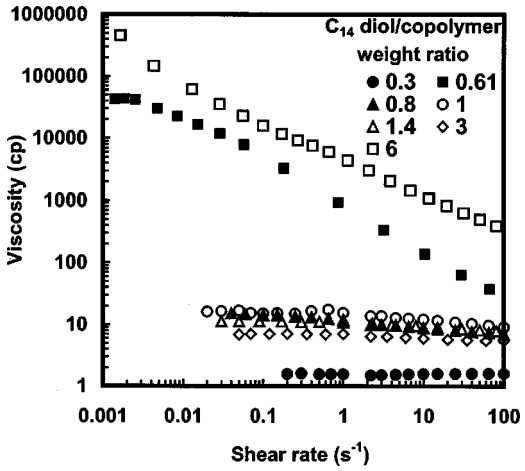

FIG. 2. Shear rate dependence of apparent viscosity for 5 wt % $(EO)_{37}(PO)_{56}(EO)_{37}$ solution with the addition of C_{14} diol at different levels.

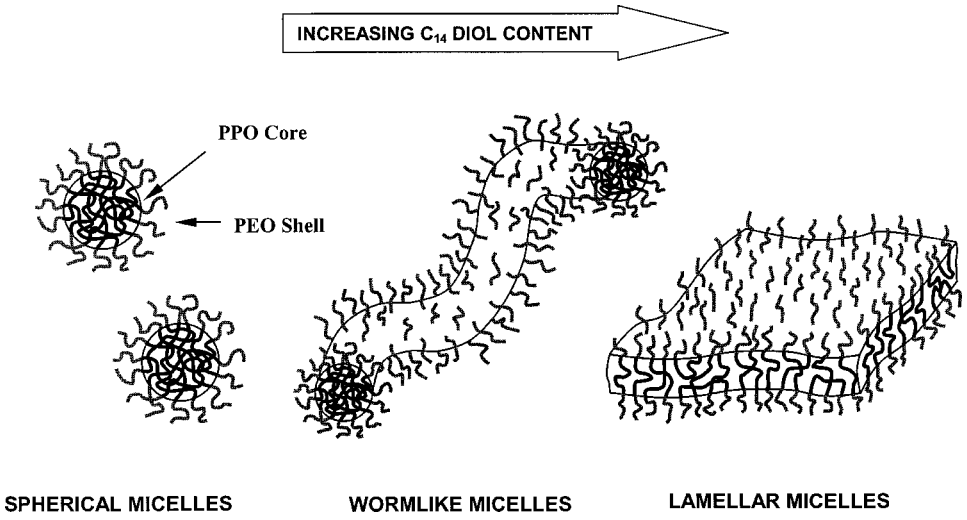

FIG. 3. Schematic representation of the cascade of micellar structure changes in copolymer solutions as C_{14} diol is added.

at the diol/copolymer weight ratio of 0.61 and 6 demonstrate strong shear thinning. This strong shear thinning is in stark contrast to the nearly Newtonian behavior at other weight ratios.

The very striking rheological changes seen in Figs. 1 and 2 are a consequence of changes in micellar structure as the hydrophobic diol is added. Later we will present SANS evidence for the cascade of structural changes shown in Fig. 3. The cascade shown in Fig. 3 is predicted [Nagarajan (1999)] to occur when an additive incorporates within the core of the micelle and has been observed experimentally in some cases [Teixeira *et al.* (2000)]. We interpret our SANS data expecting to find one of the three structures shown in Fig. 3. The form factors for these structures differ sufficiently to allow identification, *if these three structures are the only ones possible*.

SANS measurements have been made on several selected C_{14} diol/$(EO)_{37}(PO)_{56}(EO)_{37}$ solutions in D_2O. The results are shown in Fig. 4. The

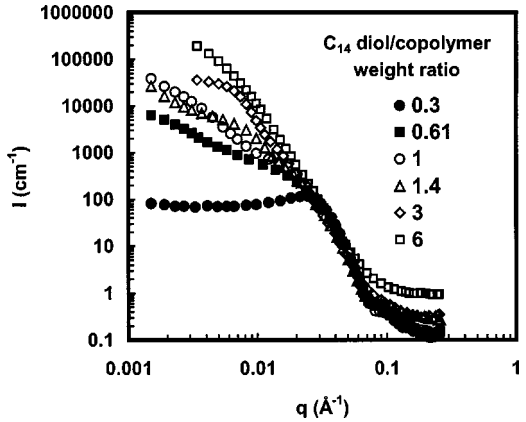

FIG. 4. Small-angle neutron scattering intensity for 5 wt % $(EO)_{37}(PO)_{56}(EO)_{37}$ solutions with added C_{14} diol at different levels.

SANS results at the diol/copolymer weight ratio of 0.3 are consistent with a microstructure of spherical micelles composed of a PPO core and PEO shell regions. This explains the almost identical solution viscosity to that of the diol-free solution. At the weight ratio of 0.61, a worm-like micelle microstructure is indicated from the scattering pattern. The local viscosity maximum as seen at this weight ratio is just the manifestation of the worm-like micelles hindered or entangled in solution. At higher diol levels, the scattering patterns are most appropriately described as lamellar and microemulsion-like (large sphere with pure diol core). In the subsequent sections, we fit the SANS intensity with known models, and explain the solution microstructure changes with increasing diol content. We assume that the C_{14} diol incorporates within the PPO core of the micelles, because the C_{14} diol partitions almost entirely into the polypropylene glycol rich phase in a ternary mixture of the C_{14} diol, polypropylene glycol, and water.

A. Spherical micelles

SANS intensity for a monodisperse system of particles can be expressed as [Hayter and Penfold (1981 and 1983); Chen (1986)],

$$I(q) = N(\Delta\rho)^2V^2P(q)S(q)+BG, \tag{1}$$

where N is the number density of scattering particles, $\Delta\rho$ is the scattering length density contrast between particle and solvent, V is the volume of an individual particle, $P(q)$ is the particle scattering form factor, $S(q)$ is the structure factor describing interparticle interactions, and BG is the incoherent background scattering. The form factor $P(q)$ for spherical micelles composed of core and shell regions is given as [Chen (1986)].

$$P(q)(\Delta\rho)^2V^2 = \left[\frac{4\pi}{3}R_1^3(\rho_1-\rho_2)\frac{3J_1(qR_1)}{qR_1}+\frac{4\pi}{3}R_2^3(\rho_2-\rho_s)\frac{3J_1(qR_2)}{qR_2}\right]^2, \tag{2}$$

where R_1 and R_2 are the core and corona radii, respectively, ρ_1 and ρ_2 are the scattering length densities of the core and corona regions, ρ_s is the scattering length density of the solvent D_2O, and $J_1(x) = (\sin x - x\cos x)/x^2$ is the first-order spherical Bessel function. In our data modeling, we assume the C_{14} diol is totally incorporated into the PPO micellar core, and the corona is D_2O-hydrated PEO. It is also reasonable to assume no water content (D_2O) in the core [Yang and Alexandridis (2000b)]. The scattering length densities of the core and the corona are, hence, given by

$$\rho_1 = \phi_{PPO}\rho_{PPO}+(1-\phi_{PPO})\rho_{diol}, \tag{3}$$

$$\rho_2 = \phi_{PEO}\rho_{PEO}+(1-\phi_{PEO})\rho_{D_2O}, \tag{4}$$

where ϕ_{PPO} and ϕ_{PEO} are the volume fraction of PPO and PEO in the core and corona of the micelles, ρ_{PPO} (0.347×10^{-6} Å^{-2}), ρ_{PEO} (0.572×10^{-6} Å^{-2}), ρ_{diol} (0.178×10^{-6} Å^{-2}), and ρ_{D_2O} (6.33×10^{-6} Å^{-2}) are the scattering length density of PPO, PEO, C_{14} diol, and D_2O, respectively. The mass density used for the calculation of volume fraction for each component is $d_{PPO} = d_{PEO} = 1.009$ g/cm^3, $d_{diol} = 0.898$ g/cm^3, and $d_{H_2O} = 1$ g/cm^3 (in the SANS measurements, D_2O was used as the solvent, with its volume fraction kept the same as that of H_2O as used for the samples in the rheological measurements).

Assuming that the steric interactions between spherical micelles can be described by the hard sphere interaction potential of the Percus–Yevick approximation, and the spatial correlation fluctuations can be described by the classical Ornstein–Zernike approxima-

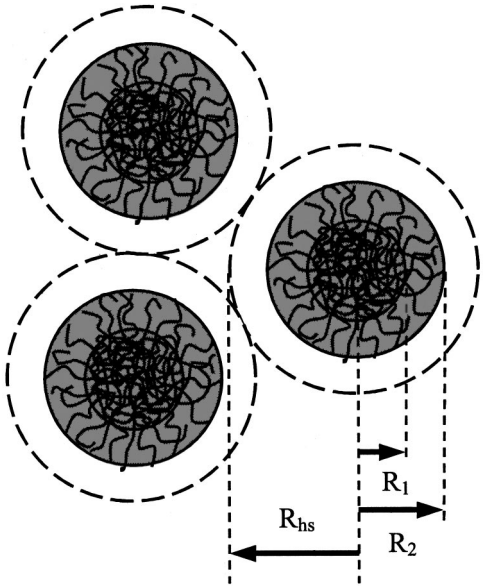

FIG. 5. Schematic of spherical micelles. R_1 and R_2 are the radii of the micelle core and shell. R_{hs} is the hard, sphere interaction radius. For relatively low copolymer concentrations, the micelles are well separated and $R_{hs} > R_2$.

tion, the structure factor $S(q)$ can be written in the following analytical format [Ashcroft and Lekner (1996); Kinning and Thomas (1984); Mortensen and Pedersen (1993b)]

$$S(q) = \frac{1}{1+24\phi G(2qR_{hs},\phi)/(2qR_{hs})}, \tag{5}$$

where $G(x,\phi)$ is a trigonometric function of $x = 2qR_{hs}$ and the volume fraction ϕ of the hard sphere of radius R_{hs} ($2R_{hs}$ is just the effective interparticle contact distance):

$$\begin{aligned} G(x,\phi) = {} & [(1+2\phi)^2/(1-\phi)^2][(\sin x - x\cos x)/x^2] - [6\phi(1+\phi/2)^2/(1-\phi)^4]\{[2x\sin x \\ & + (2-x^2)\cos x - 2]/x^3\} + [(\phi/2)(1+2\phi)^2/(1-\phi)^4]\{[4(x^3-6x) \\ & \times \sin x - (x^4-12x^2+24)\cos x + 24]/x^5\}. \end{aligned} \tag{6}$$

The micellar core and shell radii and the hard sphere radius are illustrated in Fig. 5. The significance of R_{hs} is that the micelles cannot come closer than a distance defined by $2R_{hs}$ due to strong repulsion. It should be pointed out that the volume fraction ϕ in Eq. (6) should be that of the hard spheres instead of the micelles. Only for concentrated solutions does the hard-sphere radius approach the micelle outer shell radius and the hard-sphere volume fraction converge to that of the micelles.

The earlier spherical core-shell model is fitted to the SANS data for the ternary copolymer system at the diol/copolymer weight ratio of 0.3 and the fit is shown in Fig. 6. Instrument smearing has been applied to the fit by using the resolution function $R(q,\langle q\rangle)$ developed by Pedersen and co-workers [Pedersen *et al.* (1990)]. By assuming that the C_{14} diol is totally incorporated into the PPO core and there is no water (D_2O) in the core, the volume fraction of C_{14} diol in the core region is calculated and fixed at 0.40. The core and shell radii as well as the hard-sphere interaction radius are adjustable parameters. It

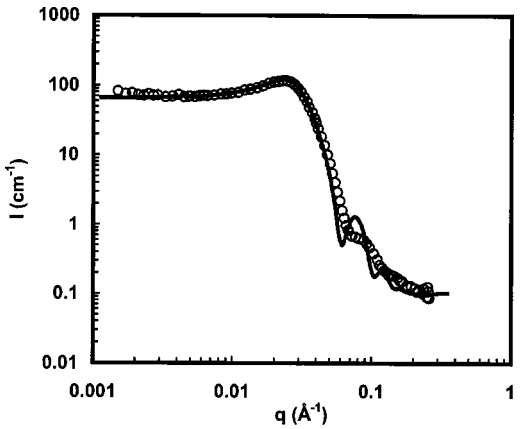

FIG. 6. SANS intensity for 5 wt % $(EO)_{37}(PO)_{56}(EO)_{37}$ solution with added C_{14} diol at a diol/copolymer weight ratio of 0.3. The smeared fit of the spherical core-shell model [solid line, Eq. (1)], gives a core radius $R_1 = 65$ Å, a shell radius $R_2 = 80$ Å, and hard sphere interaction radius $R_{hs} = 104$ Å.

is seen that the core-shell model gives a good fit to the experimental data in the low to intermediate q range. The fit generates a micellar core radius of 65 Å, a shell radius of 80 Å, and the hard-sphere interaction radius of 104 Å. The average volume fraction of PEO in the shell is thereby calculated to be 0.69. Knowing the monomer volume of PO, $V_{PO} = 95.4\,Å^3$, the micelle aggregation number is easily calculated as $n = 0.6(4\pi R_1^3/3)/(56V_{PO}) \approx 130$. A recent SANS study [Yang and Alexandridis (2000b)] reveals that 8 wt % $(EO)_{37}(PO)_{56}(EO)_{37}$ in water at 30 °C forms spherical micelles with a core radius of 40 Å, a shell radius of 71 Å, and the hard-sphere interaction radius of 84 Å. The core and shell radii increase weakly with temperature and the hard sphere interaction radius basically keeps constant as temperature is raised. The core and shell radii reach the values of 44 and 77 Å at 50 °C. The corresponding micelle aggregation number changes from ~ 50 at 30 °C to ~ 67 at 50 °C. PEO-PPO–PEO micelles usually demonstrate increased micelle size with either increased temperature or increased concentration. Our sample has lower concentration (5 wt %) and was measured at lower temperature (~ 22 °C) than Yang and Alexandridis' sample but has much larger aggregation number by a factor of almost 2. This clearly indicates that the highly hydrophobic C_{14} diol promotes aggregation of the copolymers. It is also noted that the core size of our sample has increased more than the shell size, consistent with our earlier assumption that the C_{14} diol is incorporated into the core region.

The limited smearing from the instrument resolution still leaves some wiggles in the high q range which do not fit the experimental data very well (Fig. 6). Extra smearing would be expected from two sources: polydispersity of the micelle size and smoothly decaying density profile in the corona. In our data fitting, we have assumed a sharp interface between the micelle shell and the surrounding water environment and used the simple core-shell model. In reality, the corona of hydrated PEO has a slowly varying density of monomers from the core boundary to the pure solvent water. The cap-and-gown model proposed by Liu and co-workers (1998) has a diffuse scattering length density distribution in the shell region and is expected to describe the large q data better.

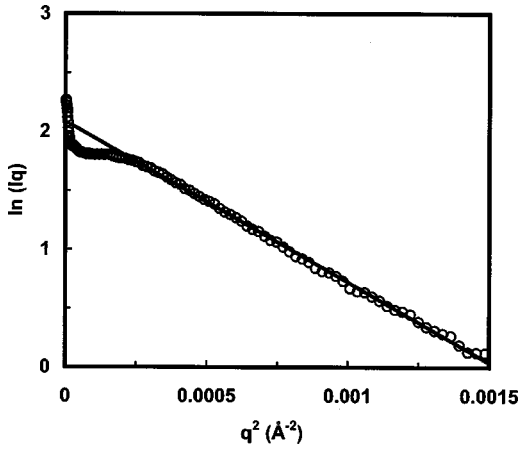

FIG. 7. Guinier plot for 5 wt % $(EO)_{37}(PO)_{56}(EO)_{37}$ in water with added C_{14} diol at a diol/copolymer weight ratio of 0.61. The cross-sectional radius of the locally rigid rod is estimated to be 72 Å from the slope of the straight line fit to Eq. (7).

B. Worm-like micelles

At the C_{14} diol/copolymer weight ratio of 0.61, which corresponds to the local viscosity maximum, the SANS pattern suggests a semiflexible wormlike micellar structure in the solution (a slope around -1 in the low q region in Fig. 4). In the large q range, the local dimension of the worm-like micelles is probed and the worm-like micelles appear rigid. The cross-sectional dimension of the locally rigid rod can be estimated as follows. For a cylindrical structure of length L and radius of the transversal cross-section R_{cyl} such that $L \gg R_{\mathrm{cyl}}$, the SANS intensity for small values of $qR_{g,c}$ where $R_{g,c} = R_{\mathrm{cyl}}/\sqrt{2}$, is the cross-sectional radius of gyration, is given by [Chen (1986); Chen and Lin (1987); Imae (1996); Imae *et al.* (1996); Okamura *et al.* (1996)]:

$$qI(q) = \pi n_p V A_t (\rho - \rho_s)^2 \exp(-R_{g,c}^2 q^2/2), \tag{7}$$

where n_p is the number density of the cylinders, $A_t = \pi R_{\mathrm{cyl}}^2$, is the area of the cross-section of the cylinder, and $V = LA_t$, is the total volume of the cylinder. A plot of $\ln(qI)$ against q^2 will give the cross-sectional radius of the cylinder from the slope of the straight line fitted to the SANS data. Such a plot for the C_{14} diol/copolymer weight ratio of 0.61 is shown in Fig. 7 and the cross-sectional radius of the locally rigid rod is estimated to be 72 Å from Eq. (7).

In order to extract information of the overall micelle dimension and the cross-section structure detail, a model fitting over the whole q range is necessary. In the model fitting, we neglect intermicellar interactions and the structure factor is taken to be $S(q) = 1$. The scattering form factor $P(q)$ for semiflexible worm-like chains in the low q regime can be modeled by the Sharp and Bloomfield approximation [Sharp and Bloomfield (1968)]

$$P_{\mathrm{SB}}(q) = \frac{2[\exp(-x)+x-1]}{x^2} + \left[\frac{4}{15} + \frac{7}{15x} - \left(\frac{11}{15} + \frac{7}{15x}\right)\exp(-x)\right]\frac{b}{L}, \tag{8}$$

where b is the Kuhn length, L is the chain contour length, and $x = q^2 R_g^2$ with R_g being the radius of gyration of the chain with excluded volume effects. Assuming the root-mean-square end-to-end distance for the flexible chain takes the form of a self-avoiding walk, $\langle R^2 \rangle^{1/2} = n^{\nu} b$, where n is the number of Kuhn segments in the chain and ν

$= 0.588$, the radius of gyration for the expanded chain can be calculated through the following formula [Doi and Edwards (1986)]:

$$R_g^2 = \frac{1}{2n^2}\sum_{\alpha=1}^{n}\sum_{\beta=1}^{n}|\alpha-\beta|^{2\nu}b^2$$

$$= \frac{1}{2n^2}\int_0^n d\alpha\int_0^n d\beta|\alpha-\beta|^{1.176}b^2$$

$$= \frac{1}{n^2}\int_0^n d\alpha\int_0^\alpha d\beta(\alpha-\beta)^{1.176}b^2$$

$$= 0.145n^{1.176}b^2 = 0.145\left(\frac{L}{b}\right)^{1.176}b^2, \tag{9}$$

The Sharp and Bloomfield approximation agrees with the correct function for $L/b > 10$ and $qb < 3.1$ to about 1% [Yamakawa and Fujii (1974); Pedersen and Schurtenberger (1996)]. At higher q values, a crossover from the Sharp and Bloomfield approximation to the rod scattering function is accomplished by means of a simple empirical crossover function. For an assembly of disordered, monodisperse cylindrical objects with radius R and length L, the scattering intensity can be written as [Herbst *et al.* (1993)]

$$I(q) = 4\pi N(\Delta\rho)^2\frac{V^2}{qL}\left(\frac{J_1(qR)}{qR}\right)^2. \tag{10}$$

We generalize this equation to account for a varying scattering length density profile across the cylinder radial direction. The scattering intensity for a cylindrical core-shell model can be expressed as

$$I_{\mathrm{cyl}}(q) = \pi N\frac{L}{q}\left[\pi R_1^2(\rho_1-\rho_2)\frac{2J_1(qR_1)}{qR_1}+\pi R_2^2(\rho_2-\rho_s)\frac{2J_1(qR_2)}{qR_2}\right]^2, \tag{11}$$

where N is the number density of the cylinders of length L, ρ_1 and ρ_2 are the scattering length density of the cylinder core and shell with radii R_1 and R_2, and ρ_s is the scattering length density of the solvent D_2O. $J_1(x)$ is the first-order Bessel function. We assume again that the C_{14} diol is totally incorporated into the core region and the shell is composed of hydrated PEO blocks. Equations (3) and (4) can then be used to calculate ρ_1 and ρ_2. The scattering intensity for the whole q range is modeled by the following equation:

$$I(q) = N(\Delta\rho)^2V^2P_{\mathrm{SB}}(q)w(qb)+I_{\mathrm{cyl}}(q)[1-w(qb)]+BG, \tag{12}$$

where $P_{\mathrm{SB}}(q)$ is given by Eq. (8) and $I_{\mathrm{cyl}}(q)$ by Eq. (11). In the low q regime, SANS probes large length scales and the cylinders are seen as thin flexible chains. The difference between the core and shell can be neglected and a uniform scattering length density can be assumed. Accordingly, the volume V in Eq. (12) for the flexible chain is taken to be πR_2^2L and $(\Delta\rho)^2$ is calculated using the following relation:

$$(\Delta\rho)^2 = \left[\rho_1\frac{R_1^2}{R_2^2}+\rho_2\left(1-\frac{R_1^2}{R_2^2}\right)-\rho_s\right]^2. \tag{13}$$

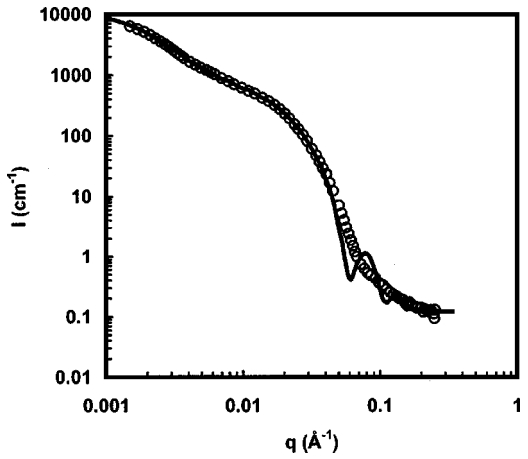

FIG. 8. SANS intensity for 5 wt % $(EO)_{37}(PO)_{56}(EO)_{37}$ solution with added C_{14} diol at a diol/copolymer weight ratio of 0.61. The solid line is the fit from the semiflexible chain model given by Eq. (12). A core radius $R_1 = 55$ Å, a shell radius $R_2 = 68$ Å, and the persistence length $1_p = 425$ Å are deduced from the fit.

The empirical crossover function $w(qb)$ in Eq. (12) is chosen as [Burchard and Kajiwara (1970); Pedersen and Schurtenberger (1996)]:

$$w(qb) = \exp[-(qb/A)^B], \tag{14}$$

where A and B are empirical constants determined by the model fit. Figure 8 shows the fit of the model given by Eq. (12) to the SANS data for our ternary mixtures at the diol/copolymer weight ratio of 0.61. A good agreement between the fit and the SANS data is achieved in the low to intermediate q range. Extra smearing from the polydispersity of the cross-sectional size of the semiflexible worm micelles and the lack of sharp interface between the shell and the surrounding water would be expected to correct the wiggles of the fit at high q values. The volume fraction of the C_{14} diol in the cylinder core is calculated first and fixed at 0.58 in the fitting process. Adjustable parameters, the core and shell radii, are deduced from the fit as 55 and 68 Å, respectively. The shell radius agrees well with the value of 72 Å as obtained previously through the Guinier analysis for the overall cross-sectional size of the locally rigid worms. Compared to the radii of the spherical micelles, the cylindrical micelles have smaller size in both the core and shell dimensions. The volume fraction of the PEO blocks in the shell is calculated as 0.79, a value significantly higher than that for the spherical micelles (0.69). The model fit leads to a persistence length of 425 Å.

In our model fitting, we have, for simplicity, neglected the intermicellar interactions and taken the structure factor $S(q)$ to be 1. With the persistence length and cylinder radius calculated above, we estimate the correlation length to be greater than 0.1 μm at the diol/copolymer weight ratio of 0.61. With such a large typical distance between worms, our assumption of $S(q) = 1$ is valid.

C. Lamellar micelles

At the diol/copolymer weight ratio of 1, the most likely micellar structure is a lamellar structure as manifested by the near -2 slope of the SANS intensity curve in the low q range (see Fig. 4). For a lamellar structure with layer thickness t, the SANS intensity at

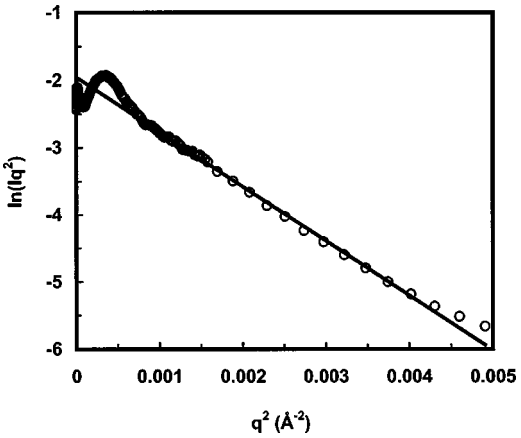

FIG. 9. Guinier plot for 5 wt % $(EO)_{37}(PO)_{56}(EO)_{37}$ in water with added C_{14} diol at a diol/copolymer weight ratio of 1. The thickness of the lamellar micelles is estimated to be $t = 99$ Å from the slope of the straight line fit to Eq. (15).

small values of $qR_{G,C}$, where $R_{G,C} = t/\sqrt{12}$, is described by the following equation [Chen (1986); Chen and Lin (1987); Imae (1996); Imae *et al.* (1996); Okamura *et al.* (1996)]:

$$q^2 I(q) = 2\pi\phi t(\rho - \rho_s)^2 \exp(-R_{G,C}^2 q^2), \tag{15}$$

where ϕ is the volume fraction of the lamellar structure in the sample. A plot according to Eq. (15) is shown in Fig. 9 for the SANS data for a diol/copolymer weight ratio of 1. The thickness of the lamellar micelles is estimated from the slope of the straight line to be $t = 99$ Å, a value much less than the diameter of both the sphere and worm structures discussed earlier.

The local structure of the lamellar arrangement of these micelles can be analyzed by model fitting the SANS data. We assume the solution to be composed of randomly distributed and oriented microdomains of parallel lamellae. Within each of the microdomains, the lamellae are stacked parallel to form layers with a preferential repeat distance. A periodic multilamellar structure of infinitely extended layers is analyzed on the basis of a periodic equation [Chen (1986); Strey *et al.* (1990)]

$$q^2 I(q) = (2\pi t^2/D)(\rho - \rho_s)^2 \left[\frac{\sin(qt/2)}{qt/2}\right]^2, \tag{16}$$

where t is the thickness of the layer, and ρ-ρ_s is the mean coherent scattering length density difference between micelle and solvent. D is the repeat distance of the layers. Equation (16) assumes a uniform scattering length density across the thickness of the layer. In our analysis, we consider a varying scattering length density across the thickness of the layer. We assume that the lamellar micelles are composed of one center PPO layer presumably incorporating the C_{14} diol and two identical outer hydrated PEO layers (see Fig. 10). We therefore generalize Eq. (16) to the following form:

$$I(q) = \frac{2\pi}{Dq^2}\left[d_2(\rho_2 - \rho_s)\frac{\sin(qd_2/2)}{qd_2/2} + d_1(\rho_1 - \rho_2)\frac{\sin(qd_1/2)}{qd_1/2}\right]^2 + BG, \tag{17}$$

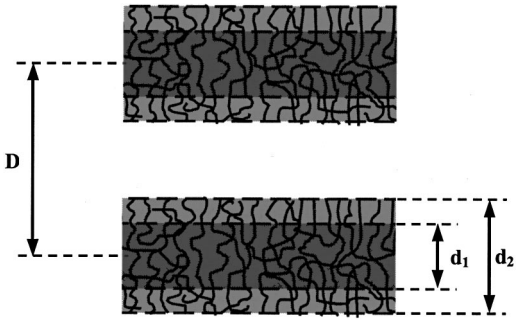

FIG. 10. Schematic of a multilayer microdomain composed of periodically stacked layers. The center layer has a thickness d_1 and the total thickness of the layer is d_2. The repeat distance of the layers is D.

where d_1 is the center layer thickness, d_2 is the total thickness of the layer, ρ_1 is the scattering length density of the center layer, ρ_2 is the scattering length density of the two outer layers, and ρ_s is the scattering length density of the solvent. BG is the incoherent background scattering. ρ_1 and ρ_2 are calculated by using Eqs. (3) and (4).

In the current analysis, we neglect intermicellar interactions and, hence, the structure factor $S(q)$ is taken to be 1. Figure 11 demonstrates the model fit according to Eq. (17) to the SANS intensity at the diol/copolymer weight ratio of 1. It is seen that the overall shape of the fit coincides with the experimental data. The deviation at q around 0.02 Å^{-1} may be interpreted as the effect of the presence of a small quantity of worm or sphere micelles. The volume fraction of PPO blocks in the center layer is calculated first and fixed as 0.308. The fit leads to a center-layer thickness $d_1 = 65\,\text{Å}$ and a total layer thickness $d_2 = 95\,\text{Å}$, a value very close to that obtained by Guinier analysis ($t = 99\,\text{Å}$ from Fig. 9). The PEO blocks account for 67% of the two outer layers according to the fit. The repeat distance D can be calculated according to the following formula:

$$\frac{d_1}{D} = \phi_{\text{diol}} + \phi_{\text{PPO}}, \tag{18}$$

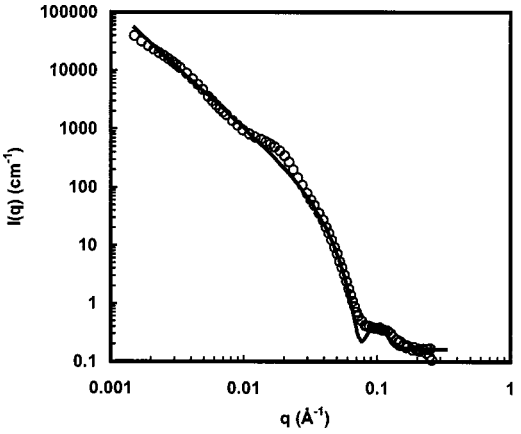

FIG. 11. SANS intensity for 5 wt % $(EO)_{37}(PO)_{56}(EO)_{37}$ solution with added C_{14} diol at a diol/copolymer weight ratio of 1. The solid line is the fit from the lamellae model Eq. (17). The center layer has a thickness $d_1 = 65\,\text{Å}$, and the total thickness of the layer is $d_2 = 95\,\text{Å}$.

where ϕ_{diol} is the volume fraction of C_{14} diol and ϕ_{PPO} the volume fraction of PPO in the solution. The calculated D is 855 Å and the corresponding Bragg peak should occur at $q_{\max} = 2\pi/D = 7.35\times10^{-3}$ Å^{-1}. As we do not observe the peak in the experimental SANS intensity around the supposed $q_{\max}$ in Fig. 11, we would say that there is no preferential repeat distance among the lamellar micelles or different microdomains have different repeat distance. This may indicate large fluctuations in these membranes [Helfrich (1978 and 1990)].

We omit the analysis for the SANS intensity at higher C_{14} diol levels due to the lack of certainty of the overall shape of the data at low q. The samples at these high diol levels are so concentrated that the neutron transmission is only 1% at the very low q range with the 12 Å neutron wavelength configuration. The scattering at this very low q range would be influenced by multiple scattering. Hence, SANS data were not taken in the very low q range for the two samples at the diol/copolymer weight ratios of 3 and 6. The higher-q data (shown in Fig. 4) are roughly consistent with a microemulsion structure with radius of order 370 Å. The interior of the microemulsion core is presumably nearly pure C_{14} diol.

To summarize, the addition of a C_{14} diol to the copolymer solutions causes the cascade of structural changes of the micelles summarized in Fig. 3. The viscosity change in Fig. 1 is the manifestation of these structural changes in solution. Up to the diol/copolymer weight ratio of 0.3 spherical micelles exist, which presumably incorporate the hydrophobic C_{14} diol into the PPO core of the micelle. This incorporation is known to lead to shape transitions of the aggregates [Nagarajan (1999)]. The first shape transition corresponds to one-dimensional growth, forming worm-like micelles. The worm-like micelles form crosslinks or entanglements and an extremely enhanced solution viscosity is observed at a diol/copolymer weight ratio of 0.61. Further addition of diol to the solution apparently induces formation of lamellar micelles that can grow two-dimensionally. Owing to the orientation of the lamellae during shear, a significantly lower solution viscosity is seen at a diol/copolymer weight ratio of 1. At diol/copolymer weight ratios above 3, the solution is a white opaque liquid without macroscopic phase separation. Since the C_{14} diol content exceeds the copolymer content in the solution, the structure in solution is most likely a large diol core enveloped by a thin copolymer corona (a microemulsion). Teixeira and co-workers have observed a similar micellar geometry transformation in aqueous solutions of SDS with the addition of decanol [Teixeira *et al.* (2000)]. At low decanol/SDS molar ratio M_d, the micelle geometry is spherical. At molar ratio $M_d = 0.20$, the micelle structure changes from spherical to cylindrical. Micellar aggregates self-assemble into cylindrical aggregates with M_d ratios of up to 0.40, where a cylinder-to-lamellar shape transition is observed. Stradner and co-workers also observed sphere-to-worm micelle transition in aqueous alkyl polyglucoside (APG) solutions upon the addition of hexanol [Stradner *et al.* (1999 and 2000)]. Hexanol acts as a ''cosurfactant'' and dissolves mainly in the interfacial layer, resulting in a structural evolution from small globular APG micelles to short cylindrical and finally giant, flexible worm-like structures. The micelle growth is one-dimensional with an unchanged local cross-sectional size.

Consistent with the concept of the interfacial curvature [Alexandridis *et al.* (1998)], $(EO)_{37}(PO)_{56}(EO)_{37}$ micelles adopt a spherical geometry at low copolymer concentration (in our case 5 wt%) due to the swelling of the PEO blocks by water molecules. The interfacial curvature is high. When the hydrophobic C_{14} diol is introduced into the solution, it incorporates within the PPO core region. This decreases the interfacial curvature due to the swelling of the PPO core by the C_{14} diol. This swelling promotes transformation of the micelles into a morphology with lower interfacial curvature. Hence, when the

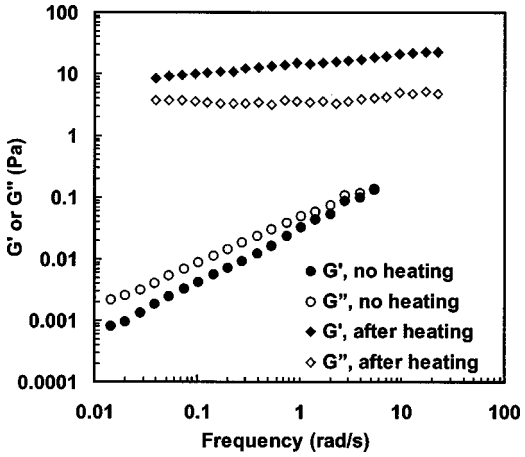

FIG. 12. Dynamic shear moduli at 20 °C for 5 wt % $(EO)_{37}(PO)_{56}(EO)_{37}$ aqueous solution with added C_{14} diol at a diol/copolymer weight ratio of 0.61, prepared at room temperature (circles). The diamonds are for data taken after the sample has been heated in the rheometer at 80 °C for 30 min and then equilibrated at 20 °C for another 30 min.

content of C_{14} diol is increased, the initial spherical micelles will develop into cylindrical and finally lamellar micelles.

D. Effect of thermal history

Thermal history affects the structure development of the C_{14} diol/copolymer mixture. Heating the sample to above 80 °C promotes the structure buildup in the solution. In order to examine thermal effects on the structure buildup in the Pluronic/Surfynol mixture, oscillatory shear experiments were carried out on a sample prepared exclusively at room temperature. The sample used was 5 wt% $(EO)_{37}(PO)_{56}(EO)_{37}$ aqueous solution with added C_{14} diol at the diol/copolymer weight ratio of 0.61, which is the state corresponding to the local maximum in viscosity shown in Fig. 1. In preparing the sample, no heating process was used and the sample was stirred for one week at room temperature before the measurement to ensure that the components in the sample were thoroughly mixed. One set of dynamic data were first taken at 20 °C. Then the sample was heated in the rheometer and maintained at 80 °C for 30 min. After the sample was cooled and equilibrated at the original temperature of 20 °C for another 30 min, a second set of dynamic data were taken. Figure 12 shows the results of these measurements. It is seen from the figure that thermal history has a huge effect on the structure buildup of the diol/copolymer mixture. Before heating, the sample has small storage and loss moduli and the loss modulus is larger than the storage modulus, suggesting the sample is a viscoelastic liquid. However, after heating to 80 °C, the viscoelastic response shows a significant increase in the two moduli as well as a larger storage than loss modulus over the range of frequency examined. This clearly indicates that the structure of the mixture depends strongly on thermal history and heating to 80 °C promotes the structure build-up. It is also noted that after the structure build-up, the dynamic moduli become less frequency dependent, with a response qualitatively similar to an elastic solid.

Steady shear measurements at low shear rate ($0.02\ s^{-1}$) were taken at different temperatures for the same sample as used for the earlier dynamic measurement. The measurements were taken at four different times after the sample preparation. The sample

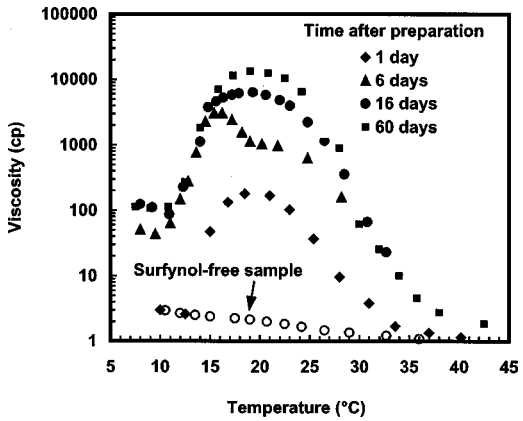

FIG. 13. Temperature dependence of viscosity at 0.02 s^{-1} for 5 wt % $(EO)_{37}(PO)_{56}(EO)_{37}$ aqueous solution with added C_{14} diol at a diol/copolymer weight ratio of 0.61 prepared at room temperature, for four different waiting times at room temperature (filled symbols). Open symbols are time-independent data for 5 wt % $(EO)_{37}(PO)_{56}(EO)_{37}$ aqueous solution without any added diol.

used for each measurement has only experienced room temperature before the measurement. During each measurement, the temperature was increased step-wise and equilibrated for 5 min before each data point was taken. The results are shown in Fig. 13. When the temperature is raised, the viscosity of the mixture has an initial small drop and then a significant increase followed by a second steady drop with temperature. Plotted in the same figure are the data for the pure stock solution of $(EO)_{37}(PO)_{56}(EO)_{37}$ at 5 wt %. The diol-free sample shows a steady decrease in viscosity with increased temperature. The data clearly demonstrate that samples at long times show the same viscosity enhancement as heat-treated samples. Hence, heat treatment accelerates the structure buildup to the equilibrium state.

VI. CONCLUSION

The increased miscibility of a C_{14} diol in water with $(EO)_{37}(PO)_{56}(EO)_{37}$ present is attributed to the incorporation of the diol into the core of the copolymer micelles. The micelle structure has been determined with SANS by assuming that the structure is either a spherical, worm-like, or lamellar micelle. Small amounts of diol simply incorporate into the existing spherical micelles without changing the micellar shape, but when enough diol is added, the micelles undergo a structural change to form worm-like micelles, accompanied by a great enhancement in solution viscosity. The worm-like micelles then transform into two-dimensional lamellar structures when more diol is added. This results in a significant drop in viscosity, presumably due to the orientation of the lamellae under shear.

Heating to 80 °C is shown to promote structure buildup in the solutions of $(EO)_{37}(PO)_{56}(EO)_{37}$ copolymer with added C_{14} diol. Since the 25 °C viscosity of the unheated solution gradually approaches that of the solution heated to 80 °C, we surmise that the heat treatment merely accelerates the system to the equilibrium state.

ACKNOWLEDGMENT

The authors thank Air Products and Chemicals, Inc. for financial support and interest in this research.

References

Alexandridis, P. and T. A. Hatton, ''Poly(ethylene oxide)-poly(propylene oxide)-poly(ethylene oxide) block copolymer surfactants in aqueous solutions and at interfaces: thermodynamics, structure, dynamics, and modeling,'' Colloids Surf., A **96**, 1–46 (1995).

Alexandridis, P., J. F. Holzwarth, and T. A. Hatton, ''Micellization of poly(ethylene oxide)-poly(propylene oxide)-poly(ethylene oxide) triblock copolymers in aqueous solutions: Thermodynamics of copolymer association,'' Macromolecules **27**, 2414–2425 (1994).

Alexandridis, P., R. Ivanova, and B. Lindman, ''Effect of glycols on the self-assembly of amphiphilic block copolymers in water. 2. Glycol location in the microstructure,'' Langmuir **16**, 3676–3689 (2000).

Alexandridis, P., U. Olsson, and B. Lindman, ''A record nine different phases (four cubic, two hexagonal, and one lamellar lyotropic liquid crystalline and two micellar solutions) in a ternary isothermal system of an amphiphilic block copolymer and selective solvents (water and oil),'' Langmuir **14**, 2627–2638 (1998).

Almgren, M., J. Alsins, and P. Bahadur, ''Fluorescence quenching and excimer formation to probe the micellization of a poly(ethylene oxide) poly(propylene oxide) poly(ethylene oxide) block copolymer, as modulated by potassium fluoride in aqueous solution,'' Langmuir **7**, 446–450 (1991a).

Almgren, M., J. van Stam, C. Lindblad, P. Y. Li, P. Stilbs, and P. Bahadur, ''Aggregation of poly(ethylene oxide)-poly(propylene oxide)-poly(ethylene oxide) triblock copolymers in the presence of sodium dodecylsulfate in aqueous-solution,'' J. Phys. Chem. **95**, 5677–5684 (1991b).

Al-Saden, A. A., T. L. Whateley, and A. T. Florence, ''Poloxamer association in aqueous solution,'' J. Colloid Interface Sci. **90**, 303–309 (1982).

Ashcroft, N. W. and J. Lekner, ''Structure and resistivity of liquid metals,'' Phys. Rev. **145**, 83–145 (1966).

Bhahadur, P., K. Pandya, M. Almgren, P. Li, and P. Stilbs, ''Effect of inorganic salts on the micellar behavior of ethylene oxide-propylene oxide block copolymers in aqueous solution,'' Colloid Polym. Sci. **271**, 657–667 (1993).

Bromberg, L., M. Temchenko, and R. H. Colby, ''Interactions among hydrophobically modified polyelectrolytes and surfactants of the same charge,'' Langmuir **16**, 2609–2614 (2000).

Brown, W., K. Schillen, and S. Hvidt, ''Triblock copolymers in aqueous solution studied by static and dynamic light scattering and oscillatory shear measurements. Influence of relative block sizes,'' J. Phys. Chem. **96**, 6038–6044 (1992).

Brown, W., K. Schillen, M. Almgren, S. Hvidt, and P. Bahadur, ''Micelle and gel formation in a poly(ethylene oxide)/poly(propylene oxide)/poly(ethylene oxide) triblock copolymer in water solution. Dynamic and static light scattering and oscillatory shearmeasurements,'' J. Phys. Chem. **95**, 1850–1858 (1991).

Burchard, W. and K. Kajiwara, ''The statistics of stiff chain molecules: I. The particle scattering factor,'' Proc. R. Soc. London, Ser. A **A316**, 185–199 (1970).

Chen, S. H., ''Small angle neutron scattering studies of the structure and interaction in micellar and microemulsion systems,'' Annu. Rev. Phys. Chem. **37**, 351–399 (1986).

Chen, S. H. and T. L. Lin, ''Colloidal solutions,'' Methods Exp. Phys. **23**, 489–543 (1987).

Chu, B., ''Structure and dynamics of block copolymer colloids,'' Langmuir **11**, 414–421 (1995).

Contractor, K. and P. Bahadur, ''Interaction of PEO-PPO-PEO block copolymer with SDS in aqueous solution,'' Eur. Polym. J. **34**, 225–228 (1998).

Doi, M. and S. F. Edwards, *The Theory of Polymer Dynamics* (Oxford University Press, New York, 1986).

Guo, L., R. H. Colby, and E. L. Paulsen, ''Rheology of Pluronic solutions mixed with a non-ionic diol surfactant,'' *Proceedings of the XIIIth International Congress on Rheology*, Cambridge UK, 2000, pp. 3-304–3-306.

Hayter, J. B. and J. Penfold, ''An analytic structure factor for macroion solutions,'' Mol. Phys. **42**, 109–118 (1981).

Hayter, J. B. and J. Penfold, ''Determination of micelle structure and charge by neutron small-angle scattering,'' Colloid Polym. Sci. **261**, 1022–1030 (1983).

Hecht, E. and H. Hoffmann, ''Interaction of ABA block copolymers with ionic surfactants in aqueous solution,'' Langmuir **10**, 86–91 (1994).

Hecht, E. and H. Hoffmann, ''Kinetic and calorimetric investigations on micelle formation of block copolymers of the poloxamer type,'' Colloids Surf., A **96**, 181–197 (1995).

Hecht, E., K. Mortensen, M. Gradzielski, and H. Hoffmann, ''Interaction of ABA block copolymers with ionic surfactants: Influence on micellization and gelation,'' J. Phys. Chem. **99**, 4866–4874 (1995).

Helfrich, W., ''Steric Interaction of Fluid Membranes in Multilayer Systems,'' Z. Naturforsch. A **33a**, 305–315 (1978).

Helfrich, W., in *Liquids at Interfaces*, edited by J. Charvolin, J. F. Joanny, and J. Zinn-Justin (Elsevier Science, New York, 1990), pp. 209–237.

Herbst, L., J. Kalus, and U. Schmelzer, ''The internal structure of a rodlike micelle,'' J. Phys. Chem. **97**, 7774–7778 (1993).

Hvidt, S., E. B. Jørgensen, W. Brown, and K. Schillén, ''Micellization and gelation of aqueous solutions of a triblock copolymer studied by rheological techniques and scanning calorimetry,'' J. Phys. Chem. **98**, 12320–12328 (1994).

Imae, T., ''SANS investigation of supramolocular assemblies constructed in aqueous alkyldimethylamine oxide solutions with organic additives,'' Colloids Surf., A **109**, 291–304 (1996).

Imae, T., M. Kakitani, M. Kato, and M. Furusaka, ''Effect of organic additives or counterions on the supramolocular assembly structures constructed by amphiphiles. A small-angle neutron scattering investigation,'' J. Phys. Chem. **100**, 20051–20055 (1996).

Ivanova, R., B. Lindman, and P. Alexandridis, ''Evolution in structural polymorphism of Pluronic F127 poly-(ethylene oxide)-poly(propylene oxide) block copolymer in ternary systems with water and pharmaceutically acceptable organic solvents: From 'glycols' to ''oils,'' '' Langmuir **16**, 9058–9069 (2000a).

Ivanova, R., B. Lindman, and P. Alexandridis, ''Effect of glycols on the self-assembly of amphiphilic block copolymers in water. 1. Phase diagrams and structure identification,'' Langmuir **16**, 3660–3675 (2000b).

Jørgensen, E. B., S. Hvidt, W. Brown, and K. Schillén, ''Effects of salts on the micellization and gelation of a triblock copolymer studied by rheology and light scattering,'' Macromolecules **30**, 2355–2364 (1997).

Kinning, D. J. and E. L. Thomas, ''Hard-sphere interactions between spherical domains in diblock copolymers,'' Macromolecules **17**, 1712–1718 (1984).

Liu, Y. C., S. H. Chen, and J. S. Huang, ''Small-angle neutron scattering analysis of the structure and interaction of triblock copolymer micelles in aqueous solution,'' Macromolecules **31**, 2236–2244 (1998).

Mortensen, K., ''Phase behavior of poly(ethylene oxide)-poly(propylene oxide)-poly(ethylene oxide) triblock-copolymer dissolved in water,'' Europhys. Lett. **19**, 599–604 (1992a).

Mortensen, K., W. Brown, and B. Norden, ''Inverse melting transition and evidence of 3-dimensional cubatic structure in a block-copolymer micellar system,'' Phys. Rev. Lett. **68**, 2340–2343 (1992b).

Mortensen, K. and W. Brown, ''Poly(ethylene oxide)-poly(propylene oxide)-poly(ethylene oxide) triblock copolymers in aqueous-solution-The influence of relative block size,'' Macromolecules **26**, 4128–4135 (1993a).

Mortensen, K. and J. S. Pedersen, ''Structural study on the micelle formation of poly(ethylene oxide)-poly(propylene oxide)-poly(ethylene oxide) triblock copolymer in aqueous solution,'' Macromolecules **26**, 805–812 (1993b).

Nagarajan, R. and K. Ganesh, ''Block copolymer self-assembly in selective solvents-Theory of solubilization in spherical micelles,'' Macromolecules **22**, 4312–4325 (1989a).

Nagarajan, R. and K. Ganesh, ''Block copolymer self-assembly in selective solvents-Spherical micelles with segregated cores,'' J. Chem. Phys. **90**, 5843–5856 (1989b).

Nagarajan, R., ''Solubilization of hydrocarbons and resulting aggregate shape transitions in aqueous solutions of Pluronic (PEO-PPO-PEO) block copolymers,'' Colloids Surf., B **16**, 55–72 (1999).

Okamura, H., T. Imae, K. Takagi, Y. Sawaki, and M. Furusaka, ''Small-angle neutron scattering investigation of supramolocular assemblies in ternary systems of alkyldimethylamine oxide/cinnamic acid/water,'' J. Colloid Interface Sci. **180**, 98–105 (1996).

Pedersen, J. S. and P. Schurtenberger, ''Scattering functions of semiflexible polymers with and without excluded volume effects,'' Macromolecules **29**, 7602–7612 (1996).

Pedersen, J. S., D. Posselt, and K. Mortensen, ''Analytical treatment of the resolution function for small-angle scattering,'' J. Appl. Crystallogr. **23**, 321–333 (1990).

Plucktaveesak, N., L. E. Bromberg, and R. H. Colby, ''Effect of surfactants on the gelation threshold temperature in aqueous solutions of a hydrophobically modified polyelectrolyte,'' Proceedings of the XIIIth International Congress on Rheology, Cambridge UK, 2000, pp. 3-307–3-309.

Prud'homme, R. K., G.-W. Wu, and D. K. Schneider, ''Structure and rheology studies of poly(oxyethylene-oxypropylene-oxyethylene) aqueous solution,'' Langmuir **12**, 4651–4659 (1996).

Sharp, P. and V. A. Bloomfield, ''Light scattering from wormlike chains with excluded volume effects,'' Biopolymers **6**, 1201–1211 (1968).

Stradner, A., B. Mayer, T. Sottmann, A. Hermetter, and O. Glatter, ''Sugar surfactant-based solutions as host systems for enzyme activity measurements,'' J. Phys. Chem. B **103**, 6680–6689 (1999).

Stradner, A., O. Glatter, and P. Schurtenberger, ''A hexanol-induced sphere-to-flexible cylinder transition in aqueous alkyl polyglucoside solutions,'' Langmuir **16**, 5354–5364 (2000).

Strey, R., R. Schomacher, D. Roux, F. Nallet, and U. Olsson, ''Dilute lamellar and L_3 phases in the binary water-$C_{12}E_5$ system,'' J. Chem. Soc., Faraday Trans. **86**, 2253–2261 (1990).

Teixeira, C. V., R. Itri, and L. Q. Amaral, ''Micellar shape transformation induced by decanol: A study by small-angle x-ray scattering (SAXS),'' Langmuir **16**, 6102–6109 (2000).

Wanka, G., H. Hoffmann, and W. Ulbricht, ''The aggregation behavior of poly-(oxyethylene)-poly-(oxypropylene)-poly-(oxyethylene)-block-copolymers in aqueous solution,'' Colloid Polym. Sci. **268**, 101–117 (1990).

Wanka, G., H. Hoffmann, and W. Ulbricht, ''Phase diagrams and aggregation behavior of poly(oxyethylene)-poly(oxypropylene)-poly(oxyethylene) triblock copolymers in aqueous solutions,'' Macromolecules **27**, 4145–4159 (1994).

Yamakawa, H. and M. Fujii, ''Light scattering from wormlike chains. Determination of the shift factor,'' Macromolecules **7**, 649–654 (1974).

Yang, L. and P. Alexandridis, ''Small-angle neutron scattering investigation of the temperature-dependent aggregation behavior of the block copolymer pluronic L64 in aqueous solution,'' Langmuir **16**, 8555–8561 (2000a).

Yang, L. and P. Alexandridis, ''Polyoxyalkylene block copolymers in formamide-water mixed solvents: Micelle formation and structure studied by small-angle neutron scattering,'' Langmuir **16**, 4819–4829 (2000b).

Zhou, Z. and B. Chu, ''Light-scattering study on the association behavior of triblock polymers of ethylene-oxide and propylene-oxide in aqueous-solution,'' J. Colloid Interface Sci. **126**, 171–180 (1988).